JMEPEG (2012) 21:2713–2718
DOI: 10.1007/s11665-012-0293-1
©ASM International
1059-9495/$19.00

Numerical and Experimental Characterizations of Damping Properties of SMAs Composite for Vibration Control Systems

C.A. Biffi, P. Bassani, A. Tuissi, M. Carnevale, N. Lecis, A. LoConte, and B. Previtali

(Submitted March 27, 2012; in revised form June 4, 2012)

Shape memory alloys (SMAs) are very interesting smart materials not only for their shape memory and superelastic effects but also because of their significant intrinsic damping capacity. The latter is exhibited upon martensitic transformations and especially in martensitic state. The combination of these SMA properties with the mechanical and the lightweight of fiberglass-reinforced polymer (FGRP) is a promising solution for manufacturing of innovative composites for vibration suppression in structural applications. CuZnAl sheets, after laser patterning, were embedded in a laminated composite between a thick FGRP core and two thin outer layers with the aim of maximizing the damping capacity of the beam for passive vibration suppression. The selected SMA $Cu_{66}Zn_{24}Al_{10}$ at.% was prepared by vacuum induction melting; the ingot was subsequently hot-and-cold rolled down to 0.2 mm thickness tape. The choice of a copper alloy is related to some advantages in comparison with NiTiCu SMA alloys, which was tested for the similar presented application in a previous study: lower cost, higher storage modulus and consequently higher damping properties in martensitic state. The patterning of the SMA sheets was performed by means of a pulsed fiber laser. After the laser processing, the SMA sheets were heat treated to obtain the desired martensitic state at room temperature. The transformation temperatures were measured by differential scanning calorimetry (DSC). The damping properties were determined, at room temperature, on full-scale sheet, using a universal testing machine (MTS), with cyclic tensile tests at different deformation amplitudes. Damping properties were also determined as a function of the temperature on miniature samples with a dynamical mechanical analyzer (DMA). Numerical modeling of the laminated composite, done with finite element method analysis and modal strain energy approaches, was performed to estimate the corresponding total damping capacity and then compared to experimental results.

Keywords damping capacity, laminated composite, laser patterning, shape memory alloy, vibration suppression

1. Introduction

Shape memory alloys (SMAs) are smart and functional materials, very attractive in respect of some well-known positive features, such as super-elasticity and shape memory effect (Ref 1). Some of these alloys, such as NiTi- and Cu-based alloys, are also characterized by high damping properties (Ref 2–4) in the martensitic state, which are associated to high internal friction capacity of the these alloys. Combining the lightness of fiberglass and the damping properties of some SMAs seems to be a very attractive proposition for the application of composite materials in different fields, such as the vibration control and suppression for automotive, aerospace, civil (Ref 5, 6), and other dynamic applications (Ref 7–9).

Some interesting examples can be found in literature, in which mainly NiTi- or NiTi-based SMAs are proposed in the shape of wires (Ref 10) and thin sheets (Ref 11), as reinforcements of fiberglass-reinforced polymer (FGRP), thanks to their relevant intrinsic dissipative effect. In spite of many exploratory studies on potential applications of SMA alloy for passive damping applications, not many real applications have been developed. One of the main reasons for this might be the difficulty in manufacturing SMA composite materials with low residual stresses at the interface of SMA material-matrix that, in service, can allow delamination. The second important reason is the high costs of the SMA alloy for which a sufficient payback of the financial investment is obtained only with a relatively high gain of the damping capacity.

The fabrication process of the composite material using wires becomes very complex for wire positioning within the matrix as well as the metal wire element delamination.

On the contrary, the problem encountered with the sheets is the need to perform the patterning and its machining (Ref 12), which has been considered important to guarantee a good adhesion between the fiberglass and the inserted elements, as well as to avoid potential delaminating effects during the flexural vibration of the structure.

This article is an invited paper selected from presentations at the International Conference on Shape Memory and Superelastic Technologies 2011, held November 6-9, 2011, in Hong Kong, China, and has been expanded from the original presentation.

C.A. Biffi, P. Bassani, and **A. Tuissi**, National Research Council CNR, Institute for Energetics and Interphases, Corso Promessi Sposi, 29, Lecco, Italy; and **M. Carnevale, N. Lecis, A. LoConte,** and **B. Previtali**, Department of Mechanical Engineering, Politecnico di Milano, Via La Masa, 34, Milan, Italy. Contact e-mail: carlo.biffi@ieni.cnr.it.

In this study, a composite material, made of fiberglass-laminated matrix and embedded with a couple of thin patterned sheets of SMA, is studied. CuZnAl-SMA was selected as reinforcement material for the sheets to be embedded into fiberglass.

The SMA sheets before being inserted into the fiberglass-laminated matrix were patterned with elliptical holes using the laser technology. The ratio between the elliptical hole surface and the SMA sheet total surface was previously investigated by the authors (Ref 11). The selected alloy was characterized by means of calorimetric (differential scanning calorimetry—DSC) and thermo-mechanical analyses (dynamic mechanical analyzer—DMA; and universal testing machine—MTS). Then, the composite beams were tested by evaluating their total damping properties. The results were reported and compared with other SMA/FGRP composites embedded with-$Ni_{40}Ti_{50}Cu_{10}$ alloy (Ref 11). A numerical simulation approach integrating the experimental results of used SMA was applied for modeling the composite behavior.

2. Materials Preparation

Pure metals were melted by means of a vacuum induction melting furnace (Balzers VSG 10) in graphite crucible, for the production of the required alloy. The nominal atomic composition of produced SMA is $Cu_{66}Zn_{24}Al_{10}$ at.%. The ingots were hot forged, hot-and-cold rolled down to 0.2-mm-thick sheets (30-mm width and 200-mm length). Laser microcutting process was performed using a nanosecond fiber laser to pattern the SMA sheets. The process parameters, adopted during the microcutting of the different materials, are reported in Table 1. A SEM image of the laser patterning is proposed in Fig. 1 and the main dimensions are reported in Table 2. The choice of this geometry for the patterning of the SMA sheets was performed because it already guaranteed the adhesion between the metal sheet and fiberglass elements increasing the amount of SMA material requested for improving total damping capacity (Ref 11). In fact, the amount of SMA material can be considered almost proportional to the internal friction; so higher material quantity means higher damping capacity.

The manufactured CuZnAl sheets, after laser microcutting, were heat treated (750 °C for 30 min) and water quenched.

Once concluded the preparation of the SMA sheets the composite elements were assembled following the procedure reported in a previous study (Ref 11). In Fig. 2, the main structure of the composite material is depicted, where two sheets of SMA are inserted in a sandwich-like structure between bulk and external layers of epoxy fiberglass. The dimensions of the composite beams are 5-mm thickness, 25-mm width, and 200-mm length.

Table 1 Main process parameters used in laser microcutting of CuZnAl sheets

Average power	50 W
Pulse frequency	80 kHz
Shielding gas/pressure	Argon at 5 bar
Number of laser pass	2
Working distance	0.5 mm
Focal distance	60 mm
Estimated laser spot diameter	23 µm
Process speed	5 mm/s

3. SMA Characterization

The characterization of the SMAs was carried out to analyze: (i) calorimetric, mechanical and internal friction properties of the SMA elements using specimen without laser patterning; (ii) total damping capacity of the SMA/FGRP composite.

First, differential scanning calorimetric analysis was performed with a DSC (TA Instrument mod. Q100), calibrated with a standard indium reference. CuZnAl specimens, of about 10 mg in weight, were scanned at heating/cooling rates of 10 °C/min within the temperature range (10-110 °C). Internal friction properties of the SMA elements were investigated on rectangular samples (20 mm × 1 mm) by means of a DMA (TA Instruments mod. Q800) in tensile configuration with 0.05% strain amplitude at 10 Hz frequency, at heating/cooling rate of 1 °C/min.

In Fig. 3, DSC scan of CuZnAl alloy, along with a NiTiCu curve, is presented. Both the curves show typical single step martensitic transformation (MT) with transformation temperatures above room temperature. As can be observed, the peaks

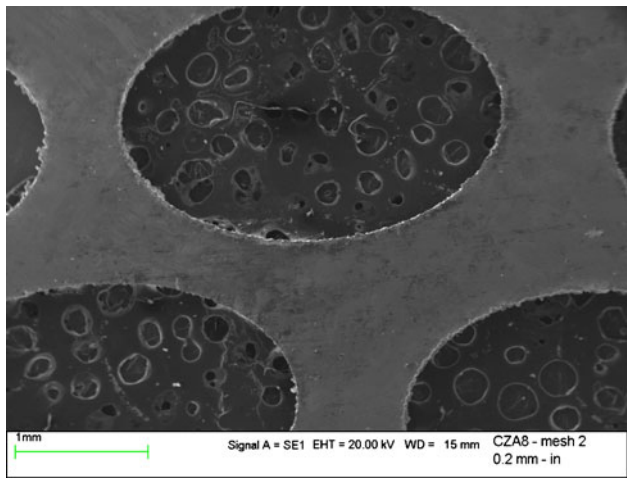

Fig. 1 SEM magnification of the laser patterning on CuZnAl

Table 2 Main dimensions of the elliptical pattern

Major semiaxis, mm	Minor semiaxis, mm	Major semiaxis / Minor semiaxis	Hole surface / Total surface
1.5	1	1.5	1.32

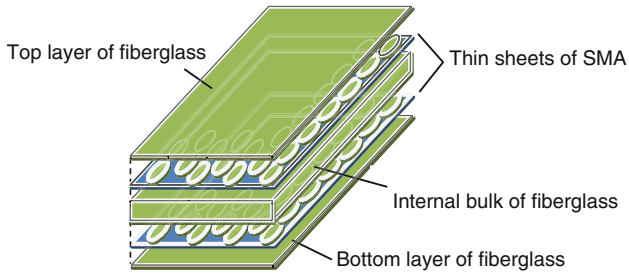

Fig. 2 Representative structure of the SMA/fiberglass composite

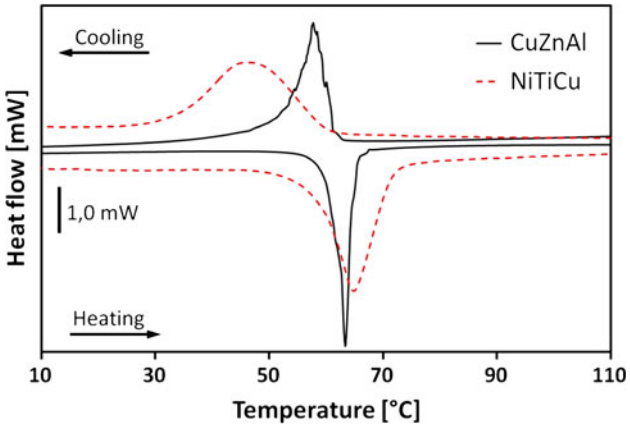

Fig. 3 DSC scan of the investigated materials

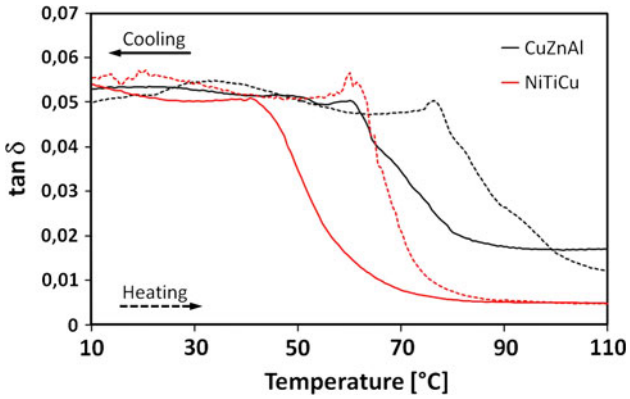

Fig. 4 DMA scan of the investigated SMAs at 0.05% strain amplitude

have shapes with sharp edges for CuZnAl, while the shapes are quite smooth for NiTiCu.

DMA scans were performed to measure the internal friction coefficient, in terms of tan δ, to serve as input data for the following numerical simulation of the composite damping properties. As shown in Fig. 4, different values of tan δ can be observed for both SMAs as a function of the temperature. Higher tan δ is associated with the martensitic state, which has to be obtained for the specific application. In the present case, tan δ is about 0.055, at 0.05% strain amplitude, for both the SMAs for temperatures less than the finishing martensitic temperature M_f.

Moreover, the damping properties of SMAs were also investigated on full-scale samples (20 mm × 200 mm) at room temperature with a MTS hydraulic machine. Stress-strain hysteresis loops were performed to measure the corresponding areas (see Fig. 5 at 0.075% strain amplitude) of the loading and the downloading steps as well as Young modulus E. The strain measurements were performed in tensile configuration using 50 mm extensometer gauge length at 0.05 Hz. During the tests, the deformation amplitude was ranging between 2×10^{-4} and 1×10^{-3}, while the minimum value is about $2–3 \times 10^{-4}$. In this characterization, no patterned sheets were tested because it was previously demonstrated that the presence of the patterning on full scale does not influence the damping properties of the alloys (Ref 11).

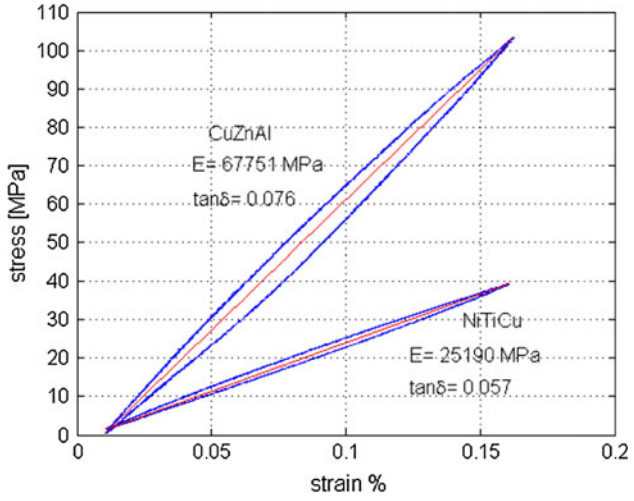

Fig. 5 Stress-strain hysteresis loop for CuZnAl and NiTiCu during MTS tensile test at 0.075% strain amplitude

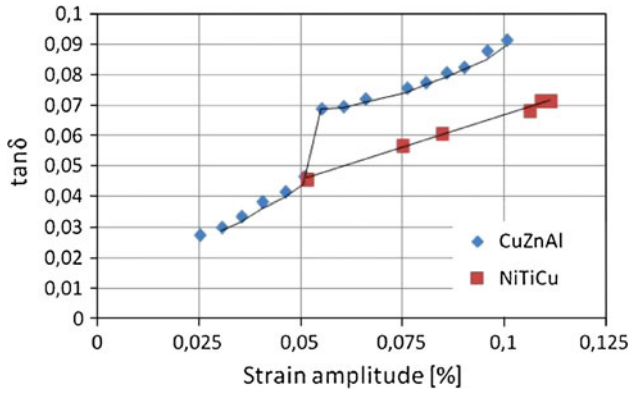

Fig. 6 Comparison between tan δ for CuZnAl and NiTiCu during MTS tensile tests

The parameter tan δ, an indicator of the internal friction property of the SMAs, is calculated as follows (see Eq 1):

$$\tan \delta_i = \frac{\Delta W_i}{2\pi W_i} \qquad \text{(Eq 1)}$$

where ΔW_i is the energy dissipated in the ith cycle of oscillation for unit volume, representing the area enclosed within the stress-strain hysteresis loop, and W_i is the maximum stored energy in the same cycle of oscillation for unit volume.

Figure 5 shows a representative stress-strain loop for the two alloys, in which Young modulus and tan δ are higher in the case of CuZnAl than in the case of NiTiCu. This trend is maintained also by varying the strain amplitude, as shown in Fig. 6. Moreover, it can be observed that tan δ increases proportionally with the strain amplitude for both the SMA alloys, as observed in a previous study (Ref 11). Each point of Fig. 6 is associated to the tan δ, measured after 10 cycles to guarantee the stabilization of the alloy behavior.

Because CuZnAl SMA alloys, compared with NiTiCu, exhibit higher storage modulus, keeping the storage modulus of the GFRP constant, they are able to store an higher percentage of specific elastic energy during the vibration of the composite. As a consequence, the composite can take the maximum

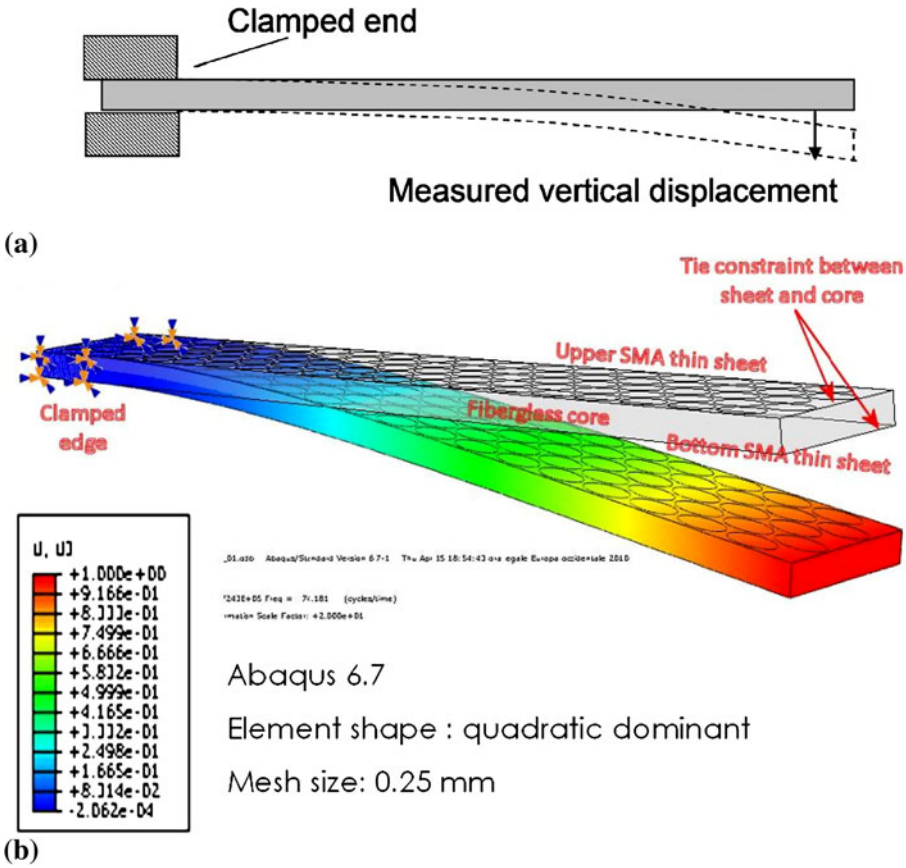

Fig. 7 Representative configuration of the flexural test (a) of the composite beam and the corresponding numerical model (b)

advantage of the higher specific damping of the CuZnAl to enhance its structural damping.

The comparison between the results obtained from DMA and MTS tests have a good agreement, considering that the sample scale is different. Nevertheless, it can be affirmed that the evaluation of tan δ is more correct from MTS measurement, due to the higher amount of material during the tensile test. Moreover, the potential errors can be distributed on all the sample scale in a better way than that occurs in DMA measurement. On the contrary, DMA analysis can suffer higher errors, because of the small amount of material involved during the test. Finally, the discontinuous trend of tan δ for CuZnAl SMA at 0.05 strain amplitude (see Fig. 6) was detected using two different types of techniques (MTS as well as DMA) on different sizes of samples, and similar trend was observed. This fact could be associated to an eventual phase transformation which is not further investigated here.

At the end, the measured values of tan δ have been used, as input data, in the next section dealing with the numerical simulation of the composite material.

4. Numerical Modeling

Damping properties of the composite beams were also evaluated using finite element method (FEM) analysis and the modal strain energy (MSE) approach, and finally these results are compared with experimental results. The MSE approach is defined by the equation as follows (see Eq 2):

$$\tan\delta = \sum_{i=1}^{N} \alpha_i \tan\delta_i \qquad \text{(Eq 2)}$$

where tan δ is the total damping of the proposed laminated composite, α_i is the ratio of elastic strain energy/total elastic energy, which is stored in each component, tan δ_i is the specific damping of each component, and N indicates the number of the components (thin SMA sheets and the matrix).

The strain energy was calculated using a linear elastic, undamped, modal finite element analysis. The FEM model of the composite was a solid model with brick elements to simulate the fiberglass core and shell elements to simulate the patterned SMA sheets. The constraint between the upper and lower surfaces of the core and the SMA sheet was a tie constraint. During the simulation, the composite beam was clamped at one end and the first flexural deformed shape was taken into account, as shown in Fig. 7(a). In Fig. 7(b), the characteristics of the used elements and mesh are reported (Ref 11). The MSE calculations are performed on an elemental basis and then summed over the fiberglass core and SMA sheets, respectively.

Table 3 proposes all the physical and mechanical properties of the investigated materials (NiTiCu, CuZnAl, fiberglass), which are requested as input data to perform the simulation of the behavior of the composite beam.

The loss factor of the composite has been calculated according to Eq 1 and with the following assumptions:

– tan δ of the CuZnAl and NiTiCu thin sheets selected from Fig. 6;

– tan δ of the fiberglass equal to 0.0084.

The loss factor (tan δ) of the oscillatory beam, considered as a single degree of freedom, when the hypothesis of viscous damping is done, and at the resonance frequency is twice the non-dimensional damping (h) of the oscillatory beam. The numerical values of the non-dimensional dampings are presented in Table 4.

The main results of the simulation, corresponding to the damping properties of the beams, made of composite material in different configurations, are presented in Table 4. In particular, Table 4 proposes the outputs from the simulation, in terms of energy stored in the SMA sheets and the fiberglass, and the estimated non-dimensional damping factor h as a function of the different configurations of the tested beams in correspondence with the first natural vibration frequency.

Thanks to the addition of SMA sheets inside the beam, a fraction of the damped elastic energy is stored in these additional elements and can take advantage from the higher damping capacity of the SMA alloy with respect to the FGRP. The elastic energy, stored by the SMA sheets, increases from 10% of the total elastic energy, when we consider NiTiCu alloy, up to 25% when we consider CuZnAl alloy. The beam with SMA-CuZnAl patterned sheets gives the better performance in terms of damping.

5. Composite Testing

The composite characterization was performed on the beams, prepared as described in Section 2. During these tests, one end of the sample was clamped, a fixed displacement was applied to the other one (see Fig. 7a), and the oscillation history of the free end vertical displacement was acquired by means of a triangulation laser. Figure 8 shows the temporal evolution of the displacement of the free end of the beam as recorded during the tests of sample with NiTiCu thin sheets embedded. As it can be observed, the displacement decreases in an exponential way and the velocity of amplitude reduction is proportional to the damping properties of the beam. Similar trends can be observed for the FGRP composite beams and for the composite beams with CuZnAl and NiTiCu inserts.

Table 3 Input data for the simulation of the composite bars

Input data	NiTiCu	CuZnAl	Glass fiber
Young modulus E, MPa	23,000	78,000	17,000
Poisson coefficient	0.30	0.20	0.35
Density, kg/mm^3	6.50×10^{-6}	7.40×10^{-6}	1.86×10^{-6}

The non-dimensional damping coefficient h can be calculated from the history of the free end displacement of the beam versus the the oscillation amplitude as follows (see Eq. 3):

$$h_n = \frac{\delta_n}{2\pi} \quad \text{where} \quad \delta_n = \ln\left(\frac{x_n}{x_{n+1}}\right) \qquad \text{(Eq 3)}$$

where δ_n is the logarithm attenuation coefficient, and x_n and x_{n+1} are the displacement amplitudes of the free end of the beam at the nth and $(n + 1)$th oscillations of the transient response, respectively.

Figure 9 shows the damping capacity of composite beams under different configurations as a function of the displacement amplitude/time. The comparison is performed between the following beams: (i) fiberglass without the SMA sheets; and (ii) patterned sheets, made of NiTiCu and CuZnAl separately, embedded in the fiberglass.

As previously shown on the basis of numerical analysis (see Table 4), Fig. 9 confirms the better performance of the CuZnAl alloy, able to improve the damping capacity of the composite material. The maximum error between numerical and experimental results is in the range of 10%.

6. Conclusions

From the present research study, the following conclusion can be drawn:

– It is possible to realize a composite material by introducing a SMA metal sheet in a glassfiber-laminated matrix overcoming the technological limits that have been outlined in a previously reported literature.

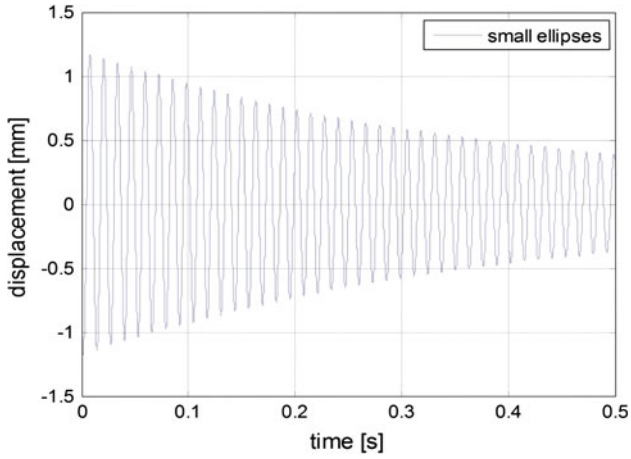

Fig. 8 Representative decay of composite beam with NiTiCu sheets in flexural configuration

Table 4 Numerical results of the composite bars at 1 mm displacement

Material	First natural frequency, Hz	Sheet elastic energy stored, %	Core elastic energy stored, %	Numerical damping of the composite h	Experimental damping of the composite h
Glass fiber	71.1	…	100	0.425	0.42
NiTiCu	74.3	10.7	89.3	0.59	0.55
CuZnAl	66.1	25	75	0.80	0.75

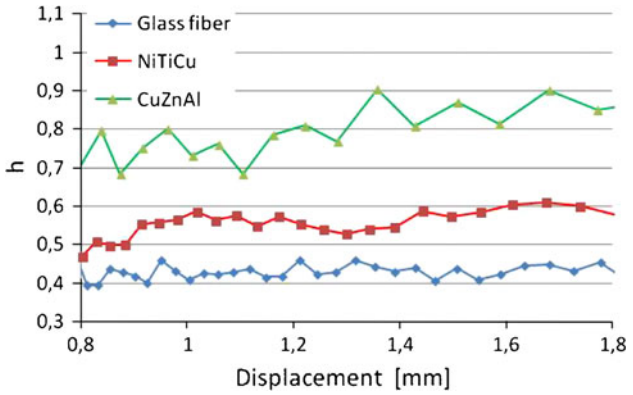

Fig. 9 Structural damping coefficient *h* in function of displacement for the investigated composite beams

– With the introduction of a metal sheet, no residual stresses at the interface have been found
– The laser patterning of the SMA sheet allows increasing the interface adhesion and avoiding composite delamination.
– In order to find the better composite damping behavior, two different SMA materials were selected: NiTiCu and CuZnAl. The storage modulus for copper alloy is higher than that of the NiTiCu one. The greater the modulus, the greater the contribution of the metal sheet under an applied load. Therefore, the copper alloy, which is more stressed, can act as more effective damping insert.
– Moreover, the copper alloy has another advantage when considered from an economical point of view, as it is cheaper than NiTiCu.

References

1. K. Otsuka and C.M. Wayman, *Shape Memory Materials*, Cambridge University Press, Cambridge, 1998
2. J. Van Humbeek and S. Kustov, Active and Passive Damping of Noise and Vibrations Through Shape Memory Alloys : Applications and Mechanisms, *Smart Mater. Struct.*, 2005, **14**, p 171–185
3. J. Van Humbeeck, Damping Capacity of Thermoelastic Martensite in Shape Memory Alloys, *J. Alloys Compd.*, 2003, **355**, p 58–64
4. A. Biscarini, B. Coluzzi, G. Mazzolai et al., Mechanical Spectroscopy of H-Free and H-Doped NiTiCu Shape Memory, *J. Alloys Compd.*, 2003, **356**, p 669–672
5. J. Salichs, Z. Hou, and M. Noori, Vibration Suppression of Structures Using Passive Shape Memory Alloy Energy Dissipation Devices, *J. Intell. Mater. Syst. Struct.*, 2001, **12**, p 671–680
6. J.C. Wilson, M. Eeri, and M.J. Wesolowsky, Shape Memory Alloys for Seismic Response Modification: A State of the Art Review, *Earthq. Spectra*, 2005, **21**, p 569–601
7. V. Torra, A. Isalgue, C. Auguet, G. Carreras, F.C. Lovey, H. Soul, and P. Terriault, Damping in Civil Engineering Using SMA. The Fatigue Behavior and Stability of CuAlBe and NiTi Alloys, *J. Mater. Eng. Perform.*, 2009, **18**(5–6), p 738–745
8. Y. Matsuzaki, T. Ikeda, and C. Boller, New Technological Development of Passive and Active Vibration Control: Analysis and Test, *Smart Mater. Struct.*, 2005, **14**, p 343–348
9. R. Zhang, Q.Q. Ni, A. Masuda, T. Yamamura, and M. Iwamoto, Vibration Characteristics of Laminated Composite Plates with Embedded Shape Memory Alloys, *Compos. Struct.*, 2006, **74**, p 389–398
10. A. Tuissi, P. Bassani, A. Casati, M. Bocciolone, A. Collina, M. Carnevale, A. Lo Conte, and B. Previtali, Application of SMA Composites in the Collectors of the Railway Pantograph for the Italian High Speed Train, *J. Mater. Eng. Perform.*, 2009, **18**, p 612–619
11. S. Arnaboldi, P. Bassani, C.A. Biffi et al., Simulated and Experimental Damping Properties of a SMA/Fiber Glass Laminated Composite, *J. Mater. Eng. Perform.*, 2011, **20**(4–5), p 551–558
12. B. Previtali, S. Arnaboldi, P. Bassani, et al., "Microcutting of NiTiCu Alloy with Pulsed Fiber Laser, ESDA 2010-24943," 10th Biennial Conference on Engineering Systems Design and Analysis, ESDA 2010, July 12–14, Istanbul